

# A regularization method for planar offset curves and bi-offset recognition

Rosanna Campagna<sup>a</sup>, Salvatore Mondrone<sup>b</sup>, Tomas Sauer<sup>c</sup>

<sup>a</sup>*Department of Mathematics and Physics, University of Campania “L. Vanvitelli”, Italy,*

<sup>b</sup>*Department of Information Engineering, Computer Science and Mathematics,  
University of L’Aquila, Italy,*

<sup>c</sup>*Lehrstuhl für Mathematik mit Schwerpunkt Digitale Bildverarbeitung & FORWISS,  
Universität Passau, Germany,*

---

## Abstract

Offset curves for planar trajectories are interesting in the generation of tool paths for numerically controlled industrial machines and in trajectory planning methods for autonomous driving systems. Theoretical offset curves may exhibit peculiar singularities, including self-intersections, which limit their use in practical applications. Existing approaches address these issue through geometric filtering techniques to detect and remove undesirable features but the computation of accurate and well-behaved offset curves remains a challenging task. We assume a first stage of functional approximation of trajectories by penalized Hermite spline regression enabling the simultaneous fitting of positions and tangents. The regularization is imposed on the second derivatives, effectively mitigating the jerk effect, which is particularly relevant in motion planning and path smoothing applications. Then, taking into account the geometrical pointwise properties of the resulting curve, we design two offset curves through the simultaneous approximation of function values and derivatives. Then, a mathematical model to obtain the so-called *bi*-offset as most fitting as with the original generator curve is proposed, also relating the offset range and pointwise curvature values. The adaptive reconstruction of the center line from the external boundaries is a topic of interest and is the main focus of our work. Numerical experiments confirm the reliability of our approach at every stage of the resolution process.

*Keywords:* Offset curves, Regression splines, Geometrical modelling, Bi-offset modeling

---

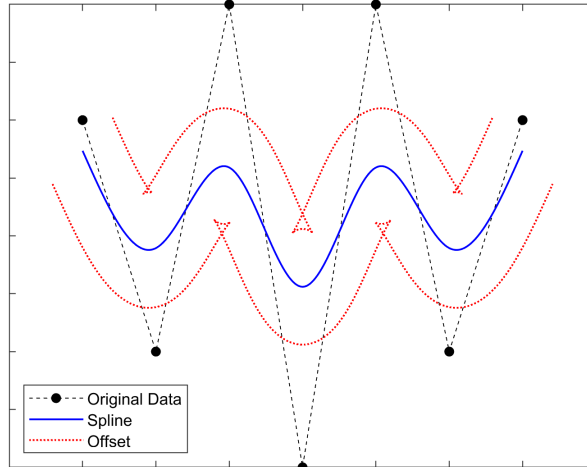


Figure 1: Cubic smoothing spline constructed on seven data points and its offsets

## 1. Introduction

The construction of offset curves for planar trajectories is a topic of widespread interest in numerous applications that require the determination of path approximations, the definition of edge trajectories, or the recognition and prediction of a path, starting from assigned or sensor-acquired control points. These examples include the generation of tool paths for industrial numerical control machines and the development of trajectory planning methods for autonomous driving systems. While the approximation of planar curves using polynomial splines of arbitrary degree under geometric continuity constraints has been widely studied, and several methodologies for offset modeling are already available in the literature [8, 9, 10, 11], the computation of accurate and well-behaved offset curves and related recognition of paths from their two offsets remain challenging tasks. Offset curves typically do not belong to the same functional space as the original trajectory. For example, the offset of a spline curve is not generally a spline itself. Moreover, offset curves may exhibit peculiar singularities, including self-intersections, which complicate their use in practical applications (see Fig. 1).

Existing approaches in the literature address these issue through geometric filtering techniques to detect and remove undesirable features [15].

Particularly [8, 10] address the offset problem, accurately reproducing both the generating curve and its offsets through approximating curves belonging to the same functional class. However, they lack the *reconstruction modeling*, which will be examined and developed in the present work. More into details, in [8], a sequence of points converging to the self-intersection of the offset curve is generated using Newton-like methods. Once the singular segment is identified in this manner, it is directly removed, thereby eliminating cusps and self-intersections. In [10], the generator is a Bézier curve. By exploiting the geometric properties of spline curves and their geometric invariance, the offsets are approximated using spline curves by setting up a least-squares problem. This formulation is derived from imposing geometric continuity conditions. The selection of the optimal parameters for the approximation follows the approach of Hoschek's studies cited in [9, 11]. In [5], the main analytical-differential properties of offset curves are outlined. In particular, characterizations of cusp points in relation to the evolute of the original curve are provided, along with the regularization property of trimmed offsets in terms of the energy integral, and the mutual distance between the offset and the generator curve. In [6], a purely algebraic study of offset curves is conducted for the case of polynomial or rational generator curves. Recalling the notion of the resultant of polynomials, it is applied to construct the implicit equations of the offset curves and to study their respective degree. A similar analysis is used to identify self-intersection points, characterized as zeros of the determinant of a modified Sylvester matrix.

In [13], a Hermite interpolation scheme is proposed to approximate offset curves when the original curve is regular, producing a polynomial representation of the offset. However, such direct approximations often fail to preserve essential characteristics of the original curve, due to the inherent nonlinearity of the offsetting operation, which involves a displacement along the normal vector field of the curve.

Recognizing these singular phenomena, which are critical in application contexts, focusing on the analytical and algebraic properties of offset curves, we introduce a new numerical model and a related algorithm for designing offset curves that are regular, smoothing, *well-performing* and useful to "coming back" to the original path.

Actually, drawing an approximation to the "offset of an offset" curve, is generally no longer able to reproduce the center-line curve from its boundaries, and it can lead to very unwanted effects and artifacts. The reason lies in the nature of the offset formation, in which the shift is made in the

direction of the normal vector. However, if the derivatives of a curve are not precisely preserved, no matter how well the values of the curve may be approximated, the offset will be faulty.

In this work, we present a regularization technique based on Hermite spline regression [2], which incorporates both function values and derivative information, enabling the simultaneous fitting of positions and tangents. The regularization is imposed on the second derivatives, effectively mitigating the jerk effect, which is particularly relevant in motion planning and path smoothing applications. Taking into account the geometrical point-wise properties of the resulting curve, we design two offset curves through the simultaneous approximation of function values and derivatives; furthermore, the contribution of the first derivative in the fitting process is modulated by a weight parameter, which is heuristically determined to balance adherence to tangent data against overall offset curve smoothness. Finally, our method allows to reconstruct an approximation of the base trajectory, given its offset curves (we say the bi-offsets, for short) that to the best of our knowledge deserve interest and not so much investigated in literature.

The paper is organized as follows: in Section 2, we introduce the definition of planar offset curve, giving basic geometrical and algebraic properties; we also analyse the nature of some critical points of the offset and their strict correspondence with the analytical character of a regular curve; Section 3 delineates a new algorithm that allows for the construction of offsets free from singularities. The proposed approach is configured with three main objectives: removal of cusp and self-intersection points relying on a non-linear regression model; obtaining offset curves that may belong to the same functional class as the generator curve (an element that is generally lost); and finally, defining a mathematical model that allows to obtain *the offset of the offset* (bi-offset) as most fitting as with the original generator curve. Some algorithmic details and remarks can be found in Section 4. Numerical experiments are in Section 5, giving results and comparative studies confirming the reliability of our approach. Conclusions and future investigations close the work.

## 2. Preliminaries

To deal with the offset definition and approximation, it is necessary to recall some preliminaries.

**Definition 1.** Let  $r : [0, 1] \rightarrow \mathbb{R}^2$  be a differentiable curve in  $\mathbb{R}^2$  defined on the compact interval  $[0, 1]$ . Then  $r$  is called a regular curve if

$$\|r'(t)\| = \sqrt{x'^2(t) + y'^2(t)} \neq 0 \quad \text{for each } t \in (0, 1).$$

**Definition 2.** Let  $r : [0, 1] \rightarrow \mathbb{R}^2$  be a regular curve, parametrically given as

$$r(t) = (x(t), y(t)), \quad t \in [a, b]$$

in the plane, and let  $\tau \neq 0$  be a fixed signed distance. The offset curve generated by  $r$  and located at a distance  $\tau$  from it is defined as:

$$r_o(t) = r(t) + \tau N(t) \quad \text{for all } t \in [0, 1],$$

where

$$N(t) = \frac{1}{\sqrt{x'(t)^2 + y'(t)^2}}(-y'(t), x'(t))$$

is the principal unit normal field to  $r(t)$  at  $t$ . We obtain an exterior or interior offset according to whether  $\tau > 0$  or  $\tau < 0$ .

To every regular unit-speed planar curve, i.e., a curve with  $\|r'\| = 1$ , two unit vector fields are associated (namely the tangent and the normal), defined as follows:

$$T(t) = r'(t), \quad N(t) = \mathcal{J}r'(t) \tag{1}$$

where the linear map  $\mathcal{J}$ , called the complex structure of  $\mathbb{R}^2$ , is

$$\mathcal{J} : (p_1, p_2) \in \mathbb{R}^2 \mapsto (-p_2, p_1) \in \mathbb{R}^2.$$

**Definition 3.** Let  $r : [0, 1] \rightarrow \mathbb{R}^2$  be a regular curve. The curvature  $k$  of  $r$  is given by the formula

$$k = \frac{r'' \cdot \mathcal{J}r'}{\|r'\|^3} \tag{2}$$

For any regular unit-speed curve in the plane, the Frenet equations are expressed as follows:

$$T' = kN, \quad N' = -kT.$$

For our purpose, it is useful to compute the tangent and normal unit vector fields associated with the offset curve. We can express the successive derivatives of  $r_o(t)$  as:

$$\begin{aligned} r'_o &= r' + \tau N' = r' + k\tau T = r' + k\tau r' = (1 + k\tau)r' \\ r''_o &= (1 + k\tau)r'' + \tau k'r', \end{aligned} \tag{3}$$

where the quantities on the right-hand sides all pertain to the generator curve  $r(t)$ . Hence, we can express the tangent and normal unit vector fields of the offset as:

$$T_o = \frac{r'_o}{\|r'_o\|} = \frac{(1+k\tau)}{|1+k\tau|}T, \quad N_o = \mathcal{J} \frac{r'_o}{\|r'_o\|} = \frac{(1+k\tau)}{|1+k\tau|}N \quad (4)$$

at the corresponding points of the offset and generator curves.

**Definition 4.** Let  $r : [0, 1] \rightarrow \mathbb{R}^2$  be a regular unit-speed curve in the plane, let  $k$  be its curvature, and let  $r_o$  be the offset curve generated by  $r$  at a fixed signed distance  $\tau$ . Then the offset curve  $r_o$  exhibits an ordinary cusp at each parameter value  $t_c$  such that:

$$k(t_c) = -\frac{1}{\tau} \quad \text{and} \quad k'(t_c) \neq 0.$$

If  $k(t) \neq -\frac{1}{\tau}$  for all  $t \in (0, 1)$ , the offset  $r_o(t)$  at distance  $\tau$  is said to be non-degenerate.

We observe that, if  $k(t_c) = -\frac{1}{\tau}$  and  $k'(t_c) \neq 0$ , then the factor  $\frac{(1+\tau k)}{|1+\tau k|}$  in the expression of the tangent and normal field of the offset is a "step function" which changes abruptly from  $-1$  to  $+1$ , or vice-versa, at  $t_c$ . The tangent  $T_o$  and the normal  $N_o$  suffer sudden inversions as we traverse such a point.

If  $r_o$  has an ordinary cusp at a parameter value  $t_c$ , we take the tangent line to the offset at that cusp to be the line through  $r_o(t_c)$  which is parallel to the tangent  $T$  of the generator at the corresponding point  $t_c$ .

Now, substituting (3) into the expression for curvature in (2), we obtain:

$$\frac{r''_o \cdot \mathcal{J}r'_o}{\|r'_o\|^3} = \frac{[(1+k\tau)r'' + \tau k'r'] \cdot (1+k\tau)\mathcal{J}r'}{(1+\tau k)^2|1+\tau k|} = \frac{k}{|1+\tau k|} \quad (5)$$

**Remark 1.** When  $k(t_e) = -\frac{1}{\tau}$  and  $k'(t_e)$  vanishes but  $k''(t_e)$  does not, the quantity

$$\frac{1+\tau k}{|1+\tau k|}$$

has the same value on either side of  $t_e$ , and therefore  $T_o$  and  $N_o$  are not inverted on passing through  $t_e$ . Although  $r_o$  has a continuous tangent at  $t_e$ , the expression for  $k_o$  indicates that the offset curvature increases without bound.

In this article, we consider only a specific class of planar curves having the form  $y = f(x)$ . The function  $f$  is assumed to be at least of class  $\mathcal{C}^2$  on its domain. We recall that a Cartesian curve can be expressed equivalently as:

$$r(t) = (t, f(t)) \quad \text{for all } t \in \text{dom } f.$$

Thus the offset curve and the curvature for a Cartesian curve are:

$$r_o(t) = \left( t - \tau \frac{f'(t)}{\sqrt{1 + f'(t)^2}}, f(t) + \tau \frac{1}{\sqrt{1 + f'(t)^2}} \right)$$

and

$$k = \frac{f''(t)}{(1 + f'(t)^2)^{3/2}}.$$

The next section presents the mathematical modeling of offset pairs starting from a functional fit of a given data set, correlated to the expected or predicted trajectory. The proposed approximation algorithm excludes the explicit computation of singular points and cusps. Instead, the procedure is framed within successive optimization problems, whose smooth regression solution is modeled through an appropriate constraint-driven minimization of the vertical distances between the points, enabling the adaptive construction of a singularity-free curve.

### 3. Offsets computation and trajectory recognition

In this section we define an algorithm that, taking into account the limits of the offsets definition, gives a smooth and meaningful offset curve, and also allows to "invert" this procedure, giving a functional form for the offset of the offset (we say *bi-offset*), as close as possible to the original functional data-driven model. One of the main issues in the reconstruction of the offset of a planar curve is that the *offset of an offset* results in a new curve, possibly far from the original generator. Fig. 2 is to show that reproducing the bi-offset, from above (*interior bi-offset*) and from below (*exterior bi-offset*), is generally not good for designing the base curve. This issue arises from the definition of the offsets, where the shift occurs along the normal vector, *without preserving the derivatives*; so, no matter how well the values of the curve may be approximated, the offset will be faulty.

Based on these considerations, we propose an algorithm designed to resolve all the aforementioned problems. The objective is to construct a model

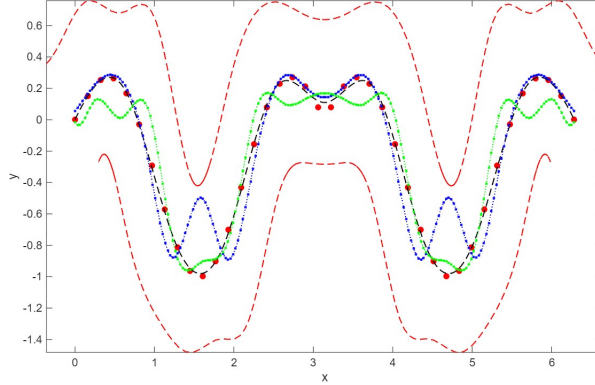


Figure 2: Base curve (black ‘•-’), computed offset at distance  $\tau = 0.5$  (red ‘- -’), interior bi-offset (blue ‘- -’), exterior bi-offset (green ‘- -’).

in which the offsetting process is *reversible*. In order to conduct a pointwise analysis of the proposed algorithm, it is appropriate to decompose the overall procedure into a sequence of well-defined steps. At each step, a regression problem must be formulated, preceded by the construction of an appropriate minimization problem. The numerical scheme will be synthesized in four steps; for any step further algorithmic and computational details will be given in the next Section 4.

To avoid redundancies in the next definitions, we preliminarily introduce some settings in the following Assumption.

**Assumption 1.** *Let consider a set of  $m$  data  $\mathcal{D} = \{(x_j, y_j)\}$ ,  $j = 1, \dots, m \in [a, b] \times \mathbb{R} \subseteq \mathbb{R}^2$  with  $a = x_1 < \dots < b = x_m$  and a basis of  $n$  B-splines  $\{B_j\}_{j=1}^n$ , of order 4, defined on an augmented set of  $n + 4$  uniformly distributed knots,  $\Xi = \{\xi_{-1}, \dots, \xi_{n+2}\}$  with  $h = \frac{b-a}{n-3}$ ,  $\xi_2 \equiv a$ ,  $\xi_{n-1} \equiv b$ ,  $\xi_{-1} < \xi_0 < \xi_1 < a$  and  $b < \xi_n < \xi_{n+1} < \xi_{n+2}$ , where the additional 6 knots are introduced in order to span the spline space  $\mathcal{S}_n$  of dimension  $n$ .*

We look for a cubic spline curve defined on the given dataset, whose definition incorporates both function and derivative constraints to better design offsets and bi-offsets.

We assume to fit the data by a regression model partially based on the same assumptions that define a P-spline, a regression model introduced in [4], and defined following [1]:

**Definition 5.** Given the **Assumption 1**, the P-spline  $s_\lambda(x) = \sum_{j=1}^n \alpha_j B_j(x)$  has coefficients that solve the penalized least square problem:

$$\min_{\alpha_1, \dots, \alpha_n} \sum_{i=1}^m \left( y_i - \sum_{j=1}^n \alpha_j B_j(x_i) \right)^2 + \lambda^2 \sum_{j=3}^n ((\Delta_2^h \boldsymbol{\alpha})_j)^2, \quad (6)$$

with the regularization parameter  $\lambda > 0$  balancing data fidelity and regularization and the penalty term defined by the difference operator on the coefficients vector  $\boldsymbol{\alpha}$ :

$$(\Delta_2^h \boldsymbol{\alpha})_j := \alpha_j - 2\alpha_{j-1} + \alpha_{j-2}, \quad j = 3, \dots, n. \quad (7)$$

The P-spline coefficients can also be seen as the solution of a Tikhonov regularization problem:

$$\min_{\boldsymbol{\alpha} \in \mathbb{R}^n} \|\mathbf{y} - \mathbf{B}\boldsymbol{\alpha}\|_2^2 + \lambda^2 \|\mathbf{D}\boldsymbol{\alpha}\|_2^2, \quad (8)$$

where  $\mathbf{y}$  is the data vector of the observed data  $\{y_i\}$ ,  $i = 1, \dots, m$ ,  $\mathbf{D} \in \mathbb{R}^{(n-2) \times n}$  is the difference three-banded matrix:

$$\mathbf{D} = \begin{bmatrix} 1 & -2 & 1 & 0 & \cdots & 0 \\ 0 & 1 & -2 & 1 & \cdots & 0 \\ \vdots & \ddots & \ddots & \ddots & \cdots & \vdots \\ \vdots & \vdots & \vdots & 1 & -2 & 1 \end{bmatrix}, \quad (9)$$

the collocation matrix of the B-splines is

$$\mathbf{B} \in \mathbb{R}^{m \times n}, \quad (\mathbf{B})_{ij} = (B_i(x_j)), \quad (10)$$

which depends on  $\{x_i\}$ ,  $i = 1, \dots, m$  and whose band structure is inherited by the locality of B-splines.

*Step 1*

In this step, we introduce a new regression spline defined as follows.

**Definition 6.** Given the **Assumption 1**, the **Trajectory Penalized spline (TP-spline)**  $g(x) = \sum_{j=1}^n \alpha_j B_j(x)$  is a modified P-spline, whose coefficients are computed by solving the following penalized least-square problem:

$$\min_{\boldsymbol{\alpha} \in \mathbb{R}^n} \|\mathbf{y} - \mathbf{B}\boldsymbol{\alpha}\|_2^2 + \mu^2 (\|\boldsymbol{\Phi}\boldsymbol{\alpha} - \Delta\mathbf{y}\|_2^2 + \|\boldsymbol{\Psi}\boldsymbol{\alpha} - \mathbf{z}\|_2^2) + \lambda^2 \|\mathbf{D}\boldsymbol{\alpha}\|_2^2, \quad (11)$$

that is

$$\begin{aligned} \min_{\alpha_1, \dots, \alpha_n} & \sum_{j=1}^N \left( \sum_{j=1}^n \alpha_j B_j(x_j) - y_j \right)^2 + \mu^2 \sum_{j=1}^N \left( \left( \sum_{j=1}^n \alpha_j B_j(x_j) \right)' - \Delta y_j \right)^2 + \\ & + \mu^2 \sum_{j=1}^N \left( \left( \sum_{j=1}^n \alpha_j B_j(x'_j) \right)' - z_j \right)^2 + \lambda^2 \sum_{j=3}^n ((\Delta_2^h \boldsymbol{\alpha})_j)^2 \end{aligned}$$

with  $\boldsymbol{\alpha}$  the vector of the spline coefficients,  $\lambda, \mu \in \mathbb{R}$  two regularization parameters,  $\mathbf{D}$  as in (9),  $\mathbf{B}$  as in (10),  $\boldsymbol{\Phi} \in \mathbb{R}^{m \times n}$ , with  $(\boldsymbol{\Phi})_{ij} = (B'_i(x_j))$ . Moreover,  $\mathbf{x}' \in \mathbb{R}^{m-1}$  is the vector of the middle points of  $\mathbf{x} \in \mathbb{R}^m$ , and  $\mathbf{z} \in \mathbb{R}^{m-1}$  is the corresponding vector of the half differences of the  $\mathbf{y} \in \mathbb{R}^m$  components; finally  $\boldsymbol{\Psi} \in \mathbb{R}^{(m-1) \times n}$ , with  $(\boldsymbol{\Psi})_{ij} = (B'_i(x'_j))$ .

The meaning of  $\mathbf{x}'$  and  $\mathbf{z}$  will be made clear in the next section. Moreover  $(\Delta \mathbf{y})_j = \frac{y_j - y_{j-1}}{x_j - x_{j-1}}$ , and  $\Delta_2^h \boldsymbol{\alpha}$  is like in (7). Differentiating the (11) with respect to  $\boldsymbol{\alpha}$  the least-square minimization problem leads to the normal equations

$$(\mathbf{B}^T \mathbf{B} + \mu^2 (\boldsymbol{\Phi}^T \boldsymbol{\Phi} + \boldsymbol{\Psi}^T \boldsymbol{\Psi}) + \lambda^2 \mathbf{D}^T \mathbf{D}) \boldsymbol{\alpha} = \mathbf{B}^T \mathbf{y} + \mu^2 (\boldsymbol{\Psi} \mathbf{z} + \boldsymbol{\Phi}^T \Delta \mathbf{y}).$$

It is worth noting that the second order discretization is introduced to suppress in  $g$  possible small, sharp hooks which are dramatically enlarged in the offset definition. Such a hook is, in fact, related to large values in the second derivative. In this phase of the algorithm we do not use any quadrature methods. Instead, we approximate the integral term using the Eilers and Marx [4] idea, with the second-order finite difference operator defined in (7).

The regularization parameters  $\mu$  and  $\lambda$  can be selected by a two-variable generalized cross-validation. This approach involves another minimization problem, in which the cost function is given by

$$h(\mu, \lambda) = \frac{\frac{1}{n} \|(I - \mathbf{H}(\mu, \lambda)) \mathbf{y}\|_2^2}{\left(1 - \frac{1}{n} \text{tr}(\mathbf{H}(\mu, \lambda))\right)^2} \quad (12)$$

where

$$\mathbf{H}(\mu, \lambda) = \mathbf{B} \mathbf{A}^{-1} \mathbf{B}^T,$$

with  $\mathbf{A} = \mathbf{B}^T \mathbf{B} + \mu^2 (\boldsymbol{\Phi}^T \boldsymbol{\Phi} + \boldsymbol{\Psi}^T \boldsymbol{\Psi}) + \lambda^2 \mathbf{D}^T \mathbf{D}$ . Once we have selected  $\mu, \lambda$  as

$$(\mu^*, \lambda^*) = \underset{\mu, \lambda > 0}{\text{argmin}} \quad h(\mu, \lambda) \quad (13)$$

we can compute the vector  $\boldsymbol{\alpha}$  by solving the linear system obtained by minimizing the (12).

*Step 2a*

Once the regression model  $g$  has been carried out, we compute the two offset curves. We cannot compute the offset ordinates directly according to the theoretical formulation. As already pointed out, the definition leads to cusps and self-intersection points. To avoid these irregularities, we define a regression model defining the offset curve by solving the problem in the following definition:

**Definition 7.** *Given the Assumption 1, the Offset Penalized spline (OP-spline)  $f$  approximating an offset curve, at a fixed distance  $\tau > 0$ , from a function  $g$ , is a regression spline  $f(x) = \sum_{j=1}^n \beta_j B_j(x)$  formulated by solving a constrained optimization problem*

$$\begin{aligned} \min \mathcal{R}(\boldsymbol{\beta}) & \tag{14} \\ \text{s.t. } f(\mathbf{x}_o) &= g(\bar{\mathbf{x}}) + \tau g^\perp(\bar{\mathbf{x}}) \\ g^\perp(\bar{\mathbf{x}}) \cdot f'(\mathbf{x}_o) &= 0. \end{aligned}$$

where  $\mathcal{R}(\boldsymbol{\beta})$  is the functional defined by:

$$\mathcal{R}(\boldsymbol{\beta}) = \int_{x_{o,\min}}^{x_{o,\max}} \|f''\|_2^2 dx, \quad f''(x) = \sum_{j=1}^n \beta_j B_j''(x).$$

and the constraints are assumed to be at any set of abscissae  $\bar{\mathbf{x}} = \{(\bar{x}_j)\}$ ,  $j = 1, \dots, q$  with the corresponding points on the offsets along the point-wise orthogonal directions, given by

$$\mathbf{x}_o^+ = \bar{\mathbf{x}} - \tau \frac{g'(\bar{\mathbf{x}})}{\sqrt{1 + g'(\bar{\mathbf{x}})^2}}.$$

It is worth noting that the methodology is analogous in both cases; for simplicity of notation we focus on the positive offset. For both, it is sufficient considering

$$\mathbf{x}_o^\pm = \bar{\mathbf{x}} \mp \tau \frac{g'(\bar{\mathbf{x}})}{\sqrt{1 + g'(\bar{\mathbf{x}})^2}}.$$

As concern with the two constraints in (14):

$$f(\mathbf{x}_o) = g(\bar{\mathbf{x}}) + \tau \frac{1}{\sqrt{1 + g'(\bar{\mathbf{x}})^2}}$$

enforces that the offset curve lies at a signed distance  $\tau$  from the generating curve, while

$$g^\perp(\bar{\mathbf{x}}) \cdot f'(\mathbf{x}_o) = 0$$

is an equivalent formulation of the parallelism condition between  $f^\perp(\mathbf{x}_o)$  and  $g^\perp(\bar{\mathbf{x}})$ .

*Step 2b (Refinement)*

In order to deduce a functional approximation of the original trajectory, starting from information about the offsets, we focus on the assumption that, at any point of the offset curve, the unit tangent vectors should have consistent orientations. We refer to this improvement as "refinement" step, and we aim to obtain an approximation of the first derivative of  $f$  that satisfies two conditions:

- (1) The tangent vectors along the two curves maintain the same orientation;
- (2) The tangent vector at each point of the offset becomes strongly proportional to the unit tangent vector at the corresponding point of the generator  $g$ .

With this aim, let  $\bar{\mathbf{x}} = \{(\bar{x}_j)\}$ ,  $j = 1, \dots, p$  be a new set of abscissae, and let  $\bar{\mathbf{x}}_o = \{(\bar{x}_{o,j})\}$ ,  $j = 1, \dots, p$  denote the abscissae for the corresponding points on the offsets along the point-wise orthogonal directions. Starting from an initial estimate for  $f$  given by Step 2a, we search for a vector  $\boldsymbol{\eta}$  such that:

$$f'(\bar{x}_{o,j}) \approx \eta_j \frac{g'(\bar{x}_j)}{\|g'(\bar{\mathbf{x}})\|_2}, \quad j = 1, \dots, p.$$

Given the coefficient vector  $\boldsymbol{\beta}$  of  $f$ , we compute the corresponding values of  $\boldsymbol{\eta}$  by solving the following nonlinear least squares problem:

$$\min_{\boldsymbol{\eta}} \sum_{j=1}^p \left( f'(\bar{x}_{o,j}) - \eta_j \frac{g'(\bar{x}_j)}{\|g'(\bar{\mathbf{x}})\|_2} \right)^2. \quad (15)$$

Step 3

In this final step, we aim to approximate the generating TP-spline, given the OP-splines refined in Step 2b:

**Definition 8.** Given the **Assumption 1**, and let  $f$  be the OP-spline of Definition 7. The **Bi-Offset spline** (BO-spline)  $h(x) = \sum_{j=1}^n \gamma_j B_j(x)$  is a regression spline, computed by solving the following nonlinear least squares problem:

$$\min_{\gamma \in \mathbb{R}^n} \|h(\bar{\mathbf{x}}_o) - g(\bar{\mathbf{x}})\|_2^2 \quad (16)$$

where  $\bar{\mathbf{x}} = \{(\bar{x}_j)\}$ ,  $j = 1, \dots, p$  is the set of points used to compute  $\boldsymbol{\eta}$ , and the abscissae for the corresponding points on the bi-offset  $h$ , along the point-wise orthogonal directions from the refinement, are given by:

$$\bar{\mathbf{x}}_0 = \bar{\mathbf{x}} - \tau \frac{\boldsymbol{\eta}^T \cdot \frac{g'(\bar{\mathbf{x}})}{\|g'(\bar{\mathbf{x}})\|_2}}{\sqrt{1 + \left(\boldsymbol{\eta}^T \cdot \frac{g'(\bar{\mathbf{x}})}{\|g'(\bar{\mathbf{x}})\|_2}\right)^2}}.$$

#### 4. Algorithmic details and insights

In this section we describe some details and computational insights in our approach.

As for the Step 1, in (11) a set of middle points  $\mathbf{x}'$  is introduced to adequately handle piecewise linear functions, for which  $\mathbf{x}$  is chosen as the 'kinks' of the function (i.e. the points where the function is not smooth, meaning its derivative is not continuous) and

$$\mathbf{x}' = \frac{1}{2} \begin{bmatrix} 1 & 1 & & \\ & \ddots & \ddots & \\ & & 1 & 1 \end{bmatrix} \mathbf{x}$$

At anyone of these average values, the derivative of the piecewise linear function is clearly defined as

$$\mathbf{z} = \frac{1}{2} \begin{bmatrix} -1 & 1 & & \\ & \ddots & \ddots & \\ & & -1 & 1 \end{bmatrix} \mathbf{y}$$

This is simpler and more stable than estimating the derivative at  $\mathbf{x}$ .

As for the Step 2a, the constrained minimization problem (14) produces an improvement in terms of curvature and imposes a strong parallelism condition between the normal direction of the generator curve at  $\bar{\mathbf{x}}$  and the normal component of the offset curve at  $\mathbf{x}_o$ . We solve (14) writing an equivalent form. For this purpose, it follows from the representation of  $f$  that:

$$\|f''\|_2^2 = \sum_{k,j} \beta_k^T \beta_j B''^{kT} B''^j.$$

Hence, the functional of the minimization problem is

$$\mathcal{R}(\boldsymbol{\beta}) = \int_{x_{\min}}^{x_{\max}} \|f''(\bar{\mathbf{x}})\|_2^2 d\bar{x} = \boldsymbol{\beta}^T \mathbf{R} \boldsymbol{\beta}$$

where,  $\mathbf{R}$  is a real symmetric matrix whose entries are given by

$$\mathbf{R}_k^j = \int_{x_{\min}}^{x_{\max}} B''(\bar{\mathbf{x}})^{kT} B''(\bar{\mathbf{x}})^j d\bar{\mathbf{x}},$$

i.e., the integral of the product of the second derivatives of the corresponding basis functions. As for the constraint  $f(\bar{\mathbf{x}}) = g(\bar{\mathbf{x}}) + \tau g^\perp(\bar{\mathbf{x}})$ , the function  $g^\perp$  represents the orthogonal component of the parametrized representation of the Cartesian curve  $g(\bar{\mathbf{x}})$ . Since the functions  $g$  and  $g^\perp$  evaluated at the set of points  $\bar{x}$  are column vectors, the constraint can be written as

$$\mathbf{B}(\bar{\mathbf{x}})\boldsymbol{\beta} = f(\bar{\mathbf{x}}) = g(\bar{\mathbf{x}}) + \tau g^\perp(\bar{\mathbf{x}}),$$

which is a linear system in the unknown  $\boldsymbol{\beta}$ .

As for the constraint  $g^\perp(\bar{\mathbf{x}}) \cdot f'(\bar{\mathbf{x}}) = 0$ , using the matrix representations, this constraint can be expressed as:

$$g^\perp(\bar{\mathbf{x}}) \cdot \mathbf{B}'(\bar{\mathbf{x}})\boldsymbol{\beta} = 0,$$

which represents a vanishing condition for the inner product of the normal vector of  $g$  and the tangent vector of  $f$ . This is a linear equation in the unknown  $\boldsymbol{\beta}$ . Based on this, a compact formulation of the constrained problem can be expressed as follows:

$$\begin{aligned} \min_{\boldsymbol{\beta}} \boldsymbol{\beta}^T \mathbf{R} \boldsymbol{\beta} & \quad (17) \\ \text{s.t. } \mathbf{A} \boldsymbol{\beta} = \mathbf{b} & \end{aligned}$$

where

$$A = \begin{bmatrix} \mathbf{B}(\bar{\mathbf{x}}) \\ g^\perp(\bar{\mathbf{x}})^T \mathbf{B}'(\bar{\mathbf{x}}) \end{bmatrix}, \quad b = \begin{bmatrix} g(\bar{\mathbf{x}}) + \tau g^\perp(\bar{\mathbf{x}}) \\ 0 \end{bmatrix}.$$

The refinement Step 2b deserves extra attention. In the previous step, we imposed a strong parallelism condition between the tangent direction of the generator and the offset curves. However, to support a *reversible* algorithm that allows us to define a derived trajectory, starting from parallelism alone is not sufficient. Even though the two tangent components have the same direction, their orientation may change and their amplitudes are not proportional. In particular, a change in orientation introduces complications in the bi-offset reconstruction problem. The idea behind the refinement is to control these issues.

Starting from (15), set  $T$  a diagonal matrix whose entries are the components of the unit tangent vector  $\frac{g'(\bar{x}_j)}{\|g'(\bar{x}_j)\|_2}$ , and given the matrix representation of the spline  $f$ , the previous problem can be expressed in an equivalent form as

$$\min_{\boldsymbol{\eta}} \|\mathbf{B}'(\bar{\mathbf{x}}_o)\boldsymbol{\beta} - T\boldsymbol{\eta}\|_2^2, \quad (18)$$

which is a quadratic minimization problem.

To compute the vector  $\boldsymbol{\eta}$ , we adopt a Conjugate Gradient method. As evidenced by the matrix formulation of the cost function:

$$\boldsymbol{\beta}^T \mathbf{H}_1 \boldsymbol{\beta} - 2\boldsymbol{\beta}^T \mathbf{f} \boldsymbol{\eta} + \boldsymbol{\eta}^T \mathbf{H}_2 \boldsymbol{\eta}$$

with  $\mathbf{H}_1 = \mathbf{B}'^T \mathbf{B}'$ ,  $\mathbf{H}_2 = \mathbf{T}^T \mathbf{T}$ , and  $\mathbf{f} = \mathbf{B}'^T \mathbf{T}$ , the optimization problem is quadratic and convex, with  $\mathbf{H}_2$  symmetric and definite positive matrix. Consequently, the minimization of this function is equivalent to finding the stationary point where the gradient vanishes. A fundamental property of this method is that, by searching along a sequence of conjugate directions, it is guaranteed to converge to the exact solution in a finite number of iterations, while it is, of course, well-known that in many cases a truly iterative application of the method often leads to better results.

In the final step, we carry out the reconstruction of the original generating curve from its offset. The main idea of this phase is to construct a new offset curve in which the upper/lower offset becomes the new generator curve. In particular, for the purpose of returning to the original curve  $g$  from the upper

offset  $f$ , we need to impose the computation of its under offset using the same fixed non-zero radius  $\tau$ . As previously remarked, it is not possible to proceed using the classical theoretical approach, thus, we engender a new regression minimum problem.

To this purpose we look for a new set of interpolating points by benefiting from the previous samples used in the refinement stage. Once computed  $\boldsymbol{\eta}$  from (18) it follows that the new set of interpolating points is given by:

$$\bar{x}_{o,j} = \bar{x}_j - \tau \frac{\eta_j g'(\bar{x}_j)}{\|g'(\bar{x}_j)\|_2} \frac{1}{\sqrt{1 + \left(\frac{\eta_j g'(\bar{x}_j)}{\|g'(\bar{x}_j)\|_2}\right)^2}},$$

and the Step 3 is reduced to solving the non-linear least-squares problem:

$$\boldsymbol{\gamma}^* = \arg \min_{\boldsymbol{\gamma}} \|h(\bar{\mathbf{x}}_o) - g(\bar{\mathbf{x}})\|_2^2 = \arg \min_{\boldsymbol{\gamma}} \|\bar{\mathbf{B}}\boldsymbol{\gamma} - g(\bar{\mathbf{x}})\|_2^2.$$

with  $\bar{\mathbf{B}} := B(\bar{\mathbf{x}}_o)$  the collocation matrix for  $h$ . It is not essential to convert this unconstrained minimum problem into a new form, it can be solved by the Matlab function `lsqnonlin`. The key element, which must be emphasized, is that the purpose of the refinement is concretely understood in the construction of the vector  $\boldsymbol{\eta}$ . This vector plays a fundamental role in the reconstruction, as it enables the construction of the new sampling - and thus the effective reconstruction - without relying on the derivatives of the released spline  $f$ , but instead adopting those of the function  $g$ . This modification is crucial, since by enforcing the derivative of  $g$  in the actual computation we prevent possible orientation inversions of  $f$ , while still preserving the same amplitude due to the carefully obtained proportionality factor. Algorithm 1 synthesizes the whole 4-step procedure.

The main issue encountered in the implementation of this algorithm lies in the non-unique and non-adaptive process for the selection and distribution of knots. Utilizing the sample data for the regression processes, the number of equidistant knots was set within a range of 20% – 40% of the sample data. This approach often produced trends that were similar to the model but exhibited undesired characteristics. We emphasize that the problem does not seem inherent to the model itself, as in regions where the knots are adequate, the process is correctly executed.

---

**Algorithm 1** TP-spline definition and bi-offset reconstruction

---

- 1: Input:
  - 2:  $\mathcal{D} = \{(x_i, y_i)\}, i = 1, \dots, m$  set of (noisy) data with  $x_i \in [a, b]$
  - 3:  $\Xi = \{\xi_{-1}, \dots, \xi_{n+2}\}$ , with  $\xi_i < \xi_{i+1}$ , uniform (augmented) set of knots with  $\xi_2 \equiv a = x_1, \xi_{n-1} \equiv b = x_m$ .
  - 4:  $B_1(x), B_2(x), \dots, B_n(x)$  cubic B-splines defined on  $\Xi$
  - 5: Step 1: Compute the TP-spline  $g(\mathbf{x})$ , by (11), with  $(\mu^*, \lambda^*)$  by (13).
  - 6: Step 2a: Construct the offsets  $f$  by (14)
  - 7: Step 2b: Refine the offsets tangent vectors by (15):
  - 8: Step 3: Construct the bi-offset function by (16).
  - 9: Output:  $h = \sum_{j=1}^n \gamma_j B_j$  be the bi-offset curve of  $g$ .
- 

An adaptive selection of knots would help make the process more streamlined, functional, and easily adaptable from one curve to another, without the need to manually set the knots correctly through a process of trial and error. Nevertheless, the penalty terms in the regression models, are generally useful for relaxing the importance of the location of the knots and their number.

## 5. Numerical Experiments

This section is to show our approach in action on different datasets. The experiments want to highlight the model reliability in the bi-offset design, the improvement given by the refinement strategy, and a comparison with classical models, available in literature.

The tests were carried out on an 13th Gen Intel(R) Core(TM) i7-13620H (2.40 GHz), 3500 MHz, 2 cores, 4 logical processors. The MATLAB<sup>©</sup> release is R2025b.

The tests reported below are performed by varying the offset distance  $\tau \in \{0.1, 0.3, 0.5, 0.7\}$ . For each radius, the theoretical offsets, the offsets constructed according to our model and the reconstruction of the base curve, with and without the application of the refinement, are referred to.

We assume to have a dataset consisting of function values and first derivatives, associated to a sequence of given abscissas. In order to simulate noisy data, zero-mean Gaussian noise is added to both the function values and the derivatives with standard deviation  $\sigma$  suitable specified. The regularization parameters  $(\mu, \lambda)$  are computed by solving a two-parameter minimization

problem, where the objective function is in (12). The (13) is solved using the Matlab `fmincon` function as a local optimizer. The minimization problem in (18) is solved using the Matlab function `pcg`.

### 5.1. Test 1 (model reliability)

In this section the experiments are to prove the model reliability, by computing the accuracy in the offset definition and in the reconstruction of the base function through the bi-offset. We consider a dataset  $(x_i, y_i)$ ,  $i = 1, \dots, 47$ , with uniformly distributed abscissae and  $y_i = p_1(x_i)$  with

$$p_1(x) = |\sin(x) \cos(2x)|, x \in [0, 2\pi].$$

We define the TP-spline using  $n = 14$  knots, and the computed regularization parameters  $\mu = 2.4628 \times 10^{-2}$  and  $\lambda = 2.0506 \times 10^{-2}$ .

In Figure 3 we describe the theoretical offsets according to the Definition 2, for different distances  $\tau$ . These results highlight the presence of cusps and self-intersections.

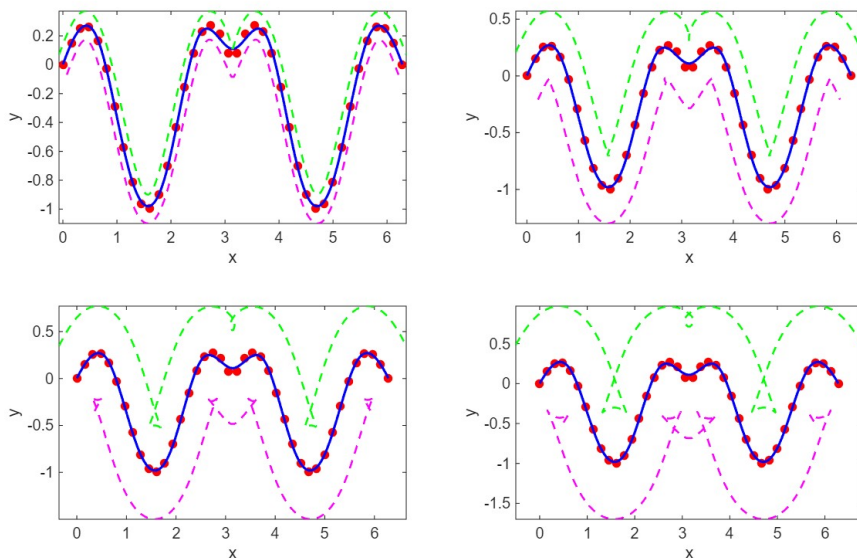


Figure 3: Base curve (blue '•-') and theoretical offsets, interior offset (magenta '△-') and exterior offset (green '○-'), for different  $\tau$ : top left  $\tau = 0.1$ , right  $\tau = 0.3$ ; bottom left  $\tau = 0.5$ , right  $\tau = 0.7$ .

In Figure 4 the two OP-splines for different distances  $\tau$  are presented. In Figure 5 we refer the comparisons between the two aforementioned ap-

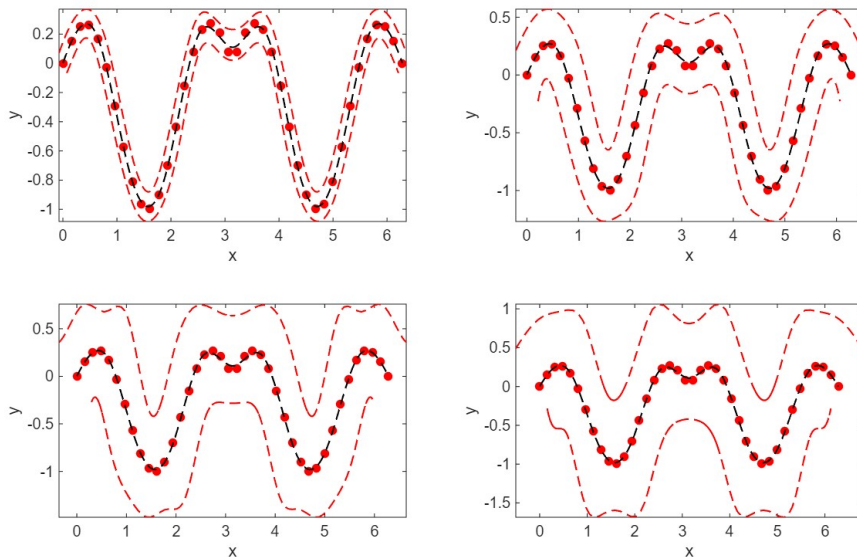


Figure 4: Base curve (black '•-') and OP-splines (red '- -') for different  $\tau$ : top left  $\tau = 0.1$ , right  $\tau = 0.3$ ; bottom left  $\tau = 0.5$ , right  $\tau = 0.7$ .

proaches, for a specific distance  $\tau = 0.3$ .

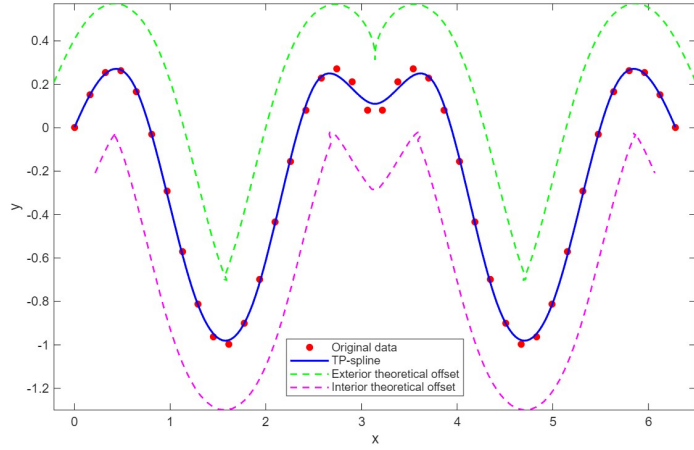
Similar results are obtained assuming data affected by relative zero-mean Gaussian noise with standard deviation  $\sigma = 10^{-2}$ . In this case the computed regularization parameters of the TP-spline are  $\lambda = 1.1086 \times 10^{-2}$  and  $\mu = 2.9283 \times 10^{-2}$  (see Figure 6).

### 5.2. Test 2 (Refinement or not refinement)

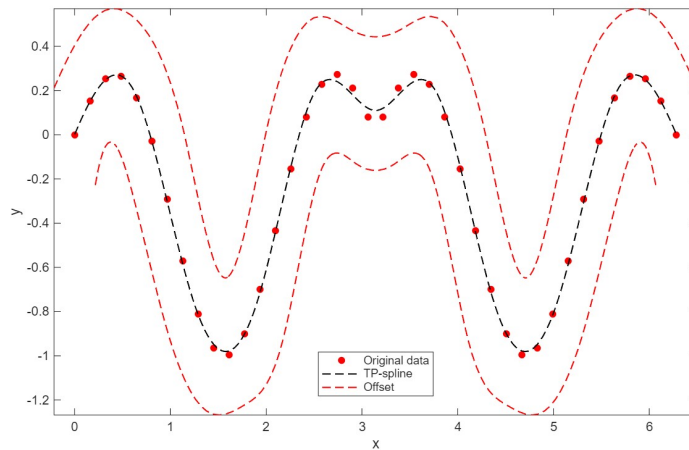
We implement this test with the aim of highlighting the improvement in bi-offsets construction using the refinement. We consider a dataset  $(x_i, y_i)$ ,  $i = 1, \dots, 51$ , with 51 uniformly distributed abscissae,  $y_i = p_2(x_i)$  with

$$p_2(x) = |\sin(x)|, x \in [-4, 4].$$

We define the TP-spline using  $n = 14$  knots, and the computed regularization parameters  $\mu = 4.3242 \times 10^{-1}$  and  $\lambda = 3.6628 \times 10^{-3}$  and compute the two BP-splines representing the two bi-offsets, respectively from below (*exterior bi-offset*) and from above (*interior bi-offset*). Figure 7 shows that the refinement



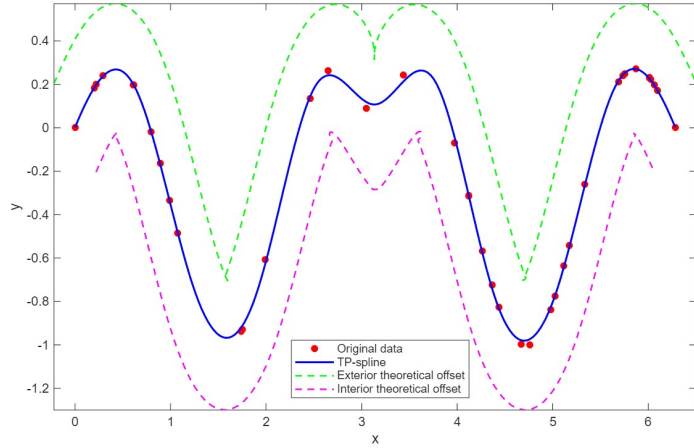
(a)



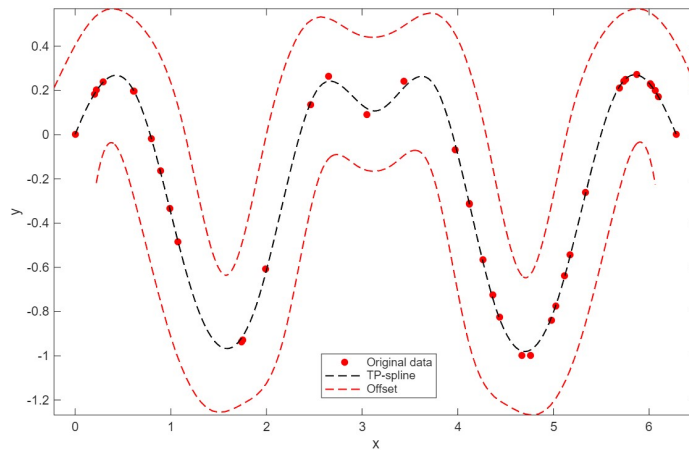
(b)

Figure 5: Case  $\tau = 0.3$ : interior (magenta '- -') and exterior (green '- -') theoretical offsets (a), OP-splines (red '- -') (b).

allows to manage the boundary effects arising in the bi-offset approximations. Numerical results confirming these improvements are detailed in the tables of the next Test section.



(a)

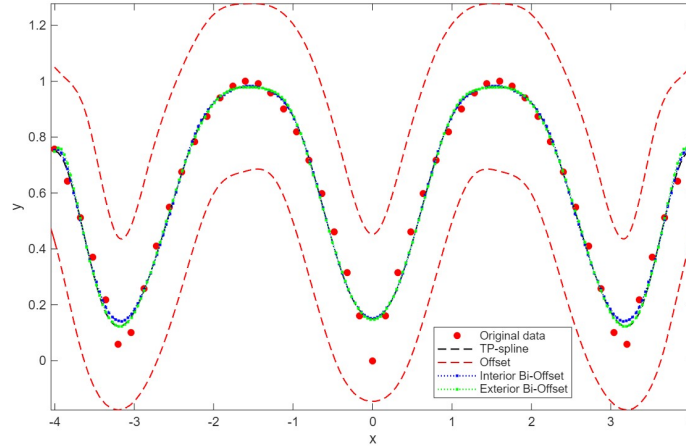


(b)

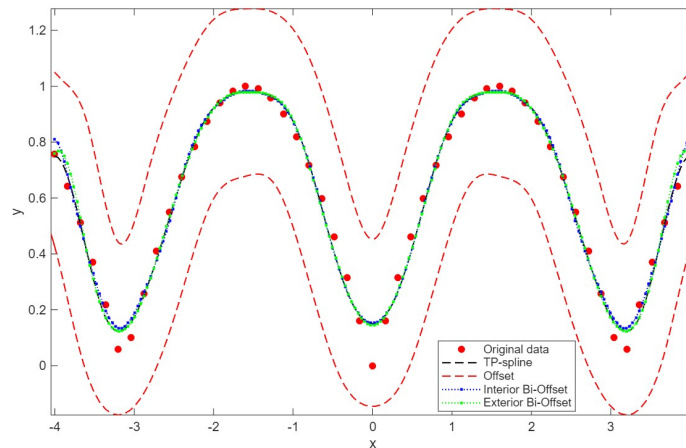
Figure 6: Case  $\tau = 0.3$ ,  $\sigma = 1.0e - 2$ : interior (magenta '- -') and exterior (green '- -') theoretical offsets (a), OP-splines (red '- -') (b).

### 5.3. Test 3 (model comparison)

This section presents some results on a comparison between the bi-offset approximations obtained both using our approach and different spline models, in the approximation of the dataset (in Step 1). Particularly we com-



(a)



(b)

Figure 7: Case  $\tau = 0.3$ : interior (or from above) (blue '-.-') and exterior (or from below) (green '-.-') BP-spline with refinement (a); interior (or from above) (blue '-.-') and exterior (or from below) BP-spline without refinement (b).

pare the results obtained by TP-spline, with the ones given by the classical P-spline [4], computed by a proprietary code, and the interpolating cubic spline, by the MATLAB function `csaps`.

In the same contexts of Test 5.1 and Test 5.2, we compute the *Mean Squared*

*Error* (MSE), quantifying the average squared deviation, between either the interior or the exterior bi-offsets with the aforementioned approximating splines, at different distances  $\tau = \{0.1, 0.3, 0.5, 0.7\}$ . The corresponding results are in the Tables 1-2 for the generating functions  $p_1(x)$  and  $p_2(x)$  respectively. We can observe that our model produces a better accuracy with respect to the compared spline models, when the approximation is given both by interior and by exterior bi-offset. Furthermore these results improve when the refinement is considered.

model	Interior <i>with refinement</i>	Interior	Exterior <i>with refinement</i>	Exterior	$\tau$
'TP-spline'	5.9752e-06	5.9072e-06	6.7020e-06	6.7080e-06	0.1
'P-spline'	5.9693e-06	5.9021e-06	6.6965e-06	6.7024e-06	0.1
'Spline'	1.2617e-04	1.2604e-04	1.2112e-04	1.2126e-04	0.1
'TP-spline'	4.1069e-04	4.2294e-04	5.7735e-04	6.7511e-04	0.3
'P-spline'	4.1045e-04	4.2268e-04	5.7696e-04	6.7481e-04	0.3
'Spline'	6.1803e-04	6.0767e-04	1.0242e-03	1.2318e-03	0.3
'TP-spline'	1.8491e-02	2.6425e-02	9.6892e-03	1.5695e-02	0.5
'P-spline'	1.8485e-02	2.6382e-02	9.6921e-03	1.5707e-02	0.5
'Spline'	2.7309e-02	3.0080e-02	1.3924e-02	2.6333e-02	0.5
'TP-spline'	1.3061e-01	1.0827e-01	4.6631e-01	5.1531e-01	0.7
'P-spline'	1.3055e-01	1.0822e-01	4.6798e-01	5.1790e-01	0.7
'Spline'	1.2021e-01	1.2386e-01	2.6408e-01	9.2787e-01	0.7

Table 1: Test function  $p_1(x) = |\sin(x) \cos(2x)|$ : Mean Square Error between the specified spline models and the computed interior and exterior bi-offsets, with and without refinement, for different  $\tau$  values.

## 6. Conclusions

In this paper we present a regularization technique which incorporates both function values and derivatives, for designing offset curves and reconstruct an approximation of the base trajectory, given its offsets (we say the bi-offsets, for short). An element of interest in the work carried out and worth to be dealt with so far is undoubtedly our model's ability to reconstruct the original curve from its offsets. The comparison metrics introduced, using the mean square error, serve to confirm the good reliability of the developed process, attesting to its functionality. Further relevance must be

model	Interior <i>with refinement</i>	Interior	Exterior <i>with refinement</i>	Exterior	$\tau$
'TP-spline'	1.0992e-06	1.4281e-06	7.0177e-07	6.3640e-07	0.1
'P-spline'	1.0721e-06	1.3217e-06	6.9827e-07	6.2982e-07	0.1
'Spline'	1.6819e-04	1.6824e-04	1.5222e-04	1.5228e-04	0.1
'TP-spline'	5.1941e-05	1.5621e-04	4.4498e-05	1.1864e-04	0.3
'P-spline'	7.5100e-05	2.5420e-04	3.1850e-05	1.0551e-04	0.3
'Spline'	2.3808e-03	2.3764e-03	1.5170e-04	1.5198e-04	0.3
'TP-spline'	5.7482e-03	1.7173e-01	3.3926e-04	8.2687e-04	0.5
'P-spline'	2.2517e-01	8.9925e-02	4.0532e-04	8.8120e-04	0.5
'Spline'	1.7940e-02	1.7965e-02	1.8115e-04	1.8096e-04	0.5
'TP-spline'	2.3323e-02	3.1002e-02	9.0385e-04	2.4493e-03	0.7
'P-spline'	3.8280e-02	3.0820e-02	1.1068e-03	2.0685e-03	0.7
'Spline'	6.9913e-02	6.9978e-02	3.6229e-04	3.6269e-04	0.7

Table 2: Test function  $p_2(x) = |\sin(x)|$ : Mean Square Error between the specified spline models and the computed interior and exterior bi-offsets, with and without refinement, for different  $\tau$  values.

given to the results concerning the relationship between the offset distance  $\tau$  and the cusps presence, connected to the curvature-radius relationship. We verify empirically that for high values of the radius, the presence of cusps increases, so attention is due to the correct choice of  $\tau$ , and drives our interest for future investigations, particularly because the selection of an optimal confidence interval or bounds for the radius, concern not only the construction of the offsets but also a regular and faithful possible extraction of road's external boundaries and adaptive reconstruction of the center line, arising in the applications of automatic or semi-automatic assisted driving [12, 14].

## Acknowledgements

RC and SM are members of the INdAM research group GNCS, which has partially supported this work. This research has been accomplished within RITA (Research ITalian network on Approximation) and UMI-TAA groups. RC was partially supported by the Italian MUR through the PRIN2022 Project 'Numerical Optimization with Adaptive Accuracy and Applications to Machine Learning', code: 2022N3ZNAX, and the PRIN2022-PNRR Project 'A multidisciplinary approach to evaluate ecosystems resilience under climate

change', code: P2022WC2ZZ.

## Declarations

The MATLAB code used in this study is available from the authors upon request.

## References

- [1] Campagna, R., Conti, C. (2021) Penalized hyperbolic-polynomial splines, *Applied Mathematics Letters*, 118.
- [2] Campagna, R., Cotronei, M., Fazzino, D. (2025) A Hermite spline model for data regression, *Mathematics and Computers in Simulation*, 229, pp. 222 - 234.
- [3] Xuejuan Chen and Qun Lin. (2014) Properties of generalized offset curves and surfaces. *Journal of Applied Mathematics*, 2014:124240.
- [4] Eilers Paul H.C. and Marx Brian D. (1986) Flexible smoothing with b-splines and penalties. *Statistical Science*, Vol. 11, No. 2, 89-121.
- [5] Farouki, R.T. and Neff, C.A. (1990) Analytic properties of plane offset curves. *Computer Aided Geometric Design*, 7(1):83–99.
- [6] Farouki, R.T. and Neff, C.A. (1990) Algebraic properties of plane offset curves. *Computer Aided Geometric Design*, 7(1):101–127.
- [7] Gray, A., Abbena, E. and Salamon S. (2006) Modern differential geometry of curves and surfaces with mathematica, *Chapman & Hall/CRC*.
- [8] Hoschek, J (1985) Offset curves in the plane. *Computer-Aided Design*, Vol. 17, Issue 2, 77-82.
- [9] Hoschek, J (1987) Approximate conversion of spline curves. *Computer Aided Geometric Design*, 4(1):59–66.
- [10] Hoschek, J (1988) Spline approximation of offset curves. *Computer Aided Geometric Design*, Vol. 5, Issue 1, 33-40.
- [11] Hoschek, J (1988) Intrinsic parametrization for approximation. *Computer Aided Geometric Design*, 5(1):27–31.

- [12] Xuemin Hu, Long Chen, Bo Tang, Dongpu Cao, and Haibo He (2018) Dynamic path planning for autonomous driving on various roads with avoidance of static and moving obstacles. *Mechanical Systems and Signal Processing*, 100:482–500.
- [13] Young Joon Ahn (2023) Hermite interpolation of offset curves of parametric regular curves. *AIMS Mathematics*, 8(12): 31008-31021.
- [14] Bai Li, Yakun Ouyang, Li Li, and Youmin Zhang (2022) Autonomous driving on curvy roads without reliance on Frenet frame: A cartesian-based trajectory planning method. *IEEE Transactions on Intelligent Transportation Systems*, 23(9):15729–15741.
- [15] Zhao, H., Zhou, L. (2017) *A Novel Method of Offset Approximation along the Normal Direction with High Precision*, Mathematical and Computational Applications, 22(3), 39.